Electronic Supplementary Information

Co_9S_8 nanoparticles encapsulated in nitrogen-doped mesoporous carbon networks with improved lithium storage properties

Jawayria Mujtaba [a, †], Hongyu Sun [*a, b, †], Guoyong Huang [c, d], Yanyan Zhao [a], Hamidreza Arandiyan [e], Guoxing Sun [f], Shengming Xu [c], Jing Zhu [*a]

[a] National Center for Electron Microscopy in Beijing, School of Materials Science and Engineering, The State Key Laboratory of New Ceramics and Fine Processing, Key Laboratory of Advanced Materials (MOE), Tsinghua University, Beijing 100084, People's Republic of China.

[b] Department of Micro- and Nanotechnology, Technical University of Denmark, 2800 Kongens Lyngby, Denmark

[c] Institute of Nuclear and New Energy Technology, Tsinghua University, Beijing 100084, China

[d] School of Metallurgy and Environment, Central South University, Changsha 410083, China

[e] Particles and Catalysis Research Group, School of Chemical Engineering, The University of New South Wales, Sydney, New South Wales 2052, Australia

[f] Department of Civil and Environmental Engineering, The Hong Kong University of Science and Technology, Hong Kong, China

[†] These authors contributed equally to this work.

[*]Corresponding authors.
E-mail address: hsun@nanotech.dtu.dk (H. Y. Sun); jzhu@mail.tsinghua.edu.cn (J. Zhu)

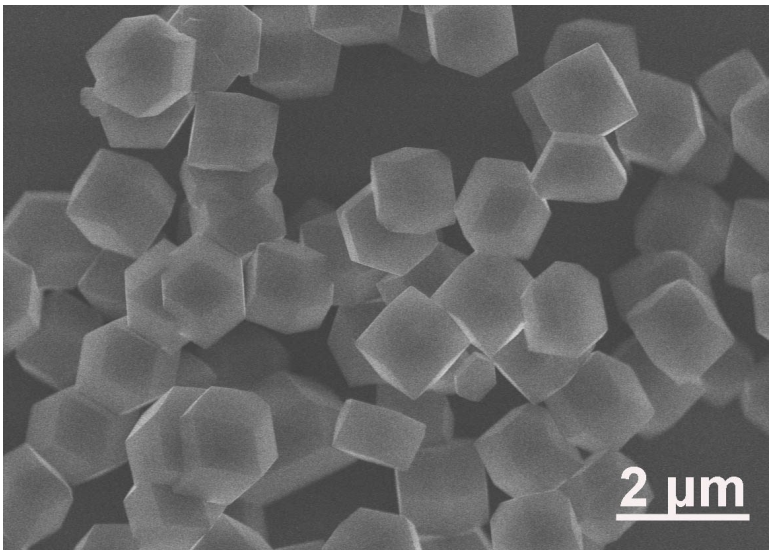

Fig. S1 Typical FESEM image of the as-prepared ZIF-67 crystals.

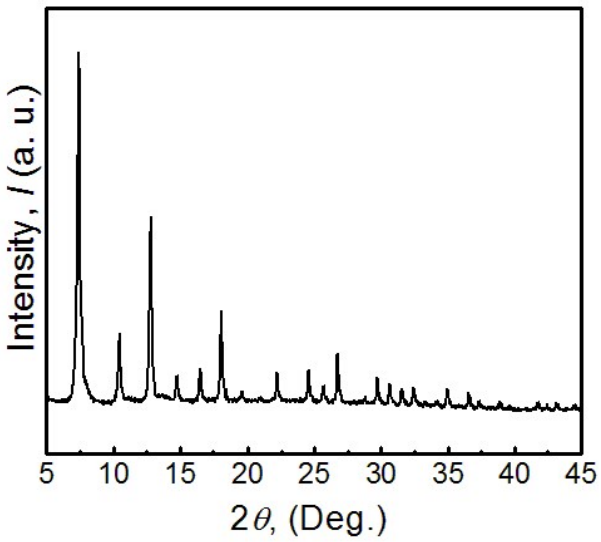

Fig. S2 XRD pattern of the as-prepared ZIF-67 crystals.

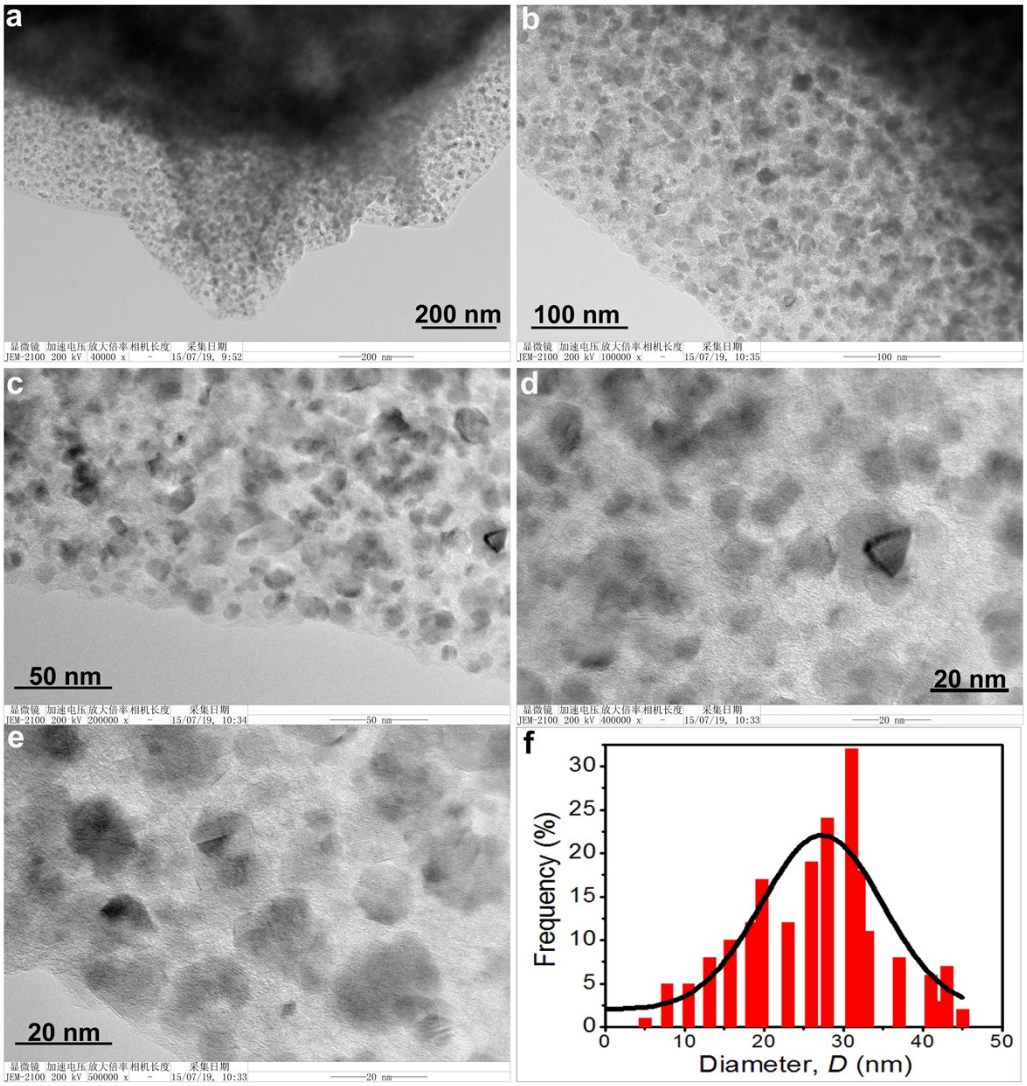

Fig. S3 (a-e) Additional TEM images of the Co_9S_8@NMCN nanocomposites, (f) size distribution histogram of Co_9S_8 nanoparticles.

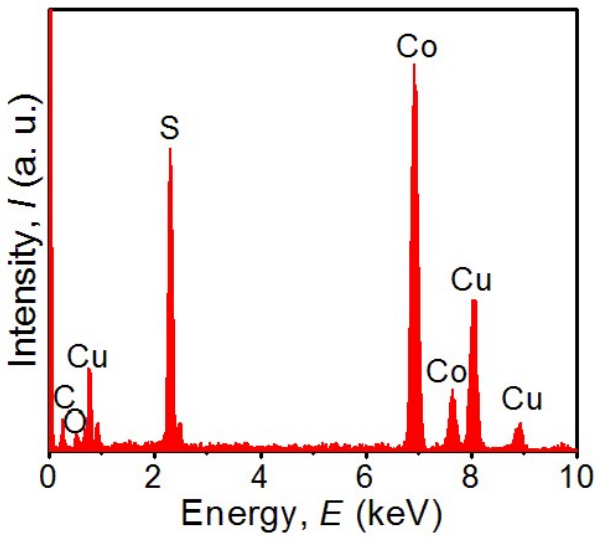

Fig. S4 EDX pattern of the Co_9S_8@NMCN nanocomposites.

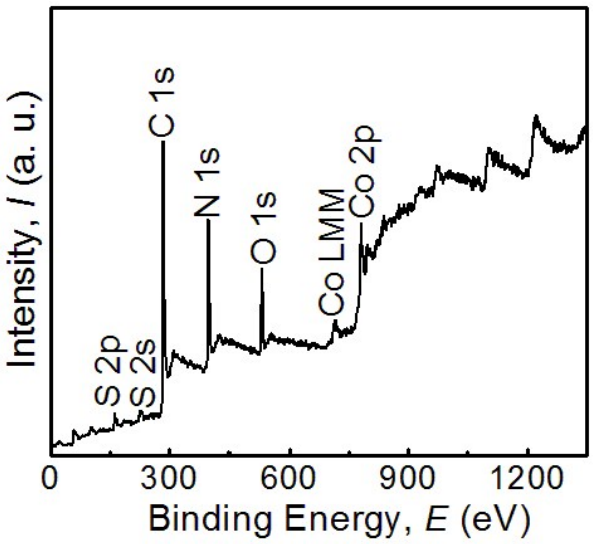

Fig. S5 XPS survey spectrum of the Co_9S_8@NMCN nanocomposites.

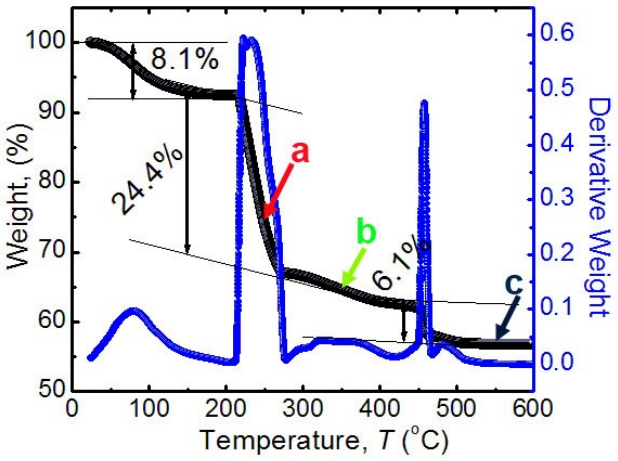

Fig. S6 Thermogravimetric TGA and DTA curves of the Co_9S_8@NMCN nanocomposites measured by using TG 2050 thermogravimetric analyzer under an air atmosphere at the temperature range of 25-600 °C with a heating rate of 10 °C min^{-1}.

The Co_9S_8@NMCN nanocomposites show a three-step mass-loss process. *Ex-situ* XRD (Fig. S7) was performed to determine the phase of the products from TGA experiments at temperatures of 250, 350, and 550 °C. A small weight loss (8.1%) from room temperature to 200 °C can be attributed to the removal of physically adsorbed water. The second weight loss (~24.4%) step between 200 °C and 450 °C is ascribed to the oxidation of Co_9S_8 into Co_3O_4, the re-crystallization of Co_3O_4 and partial combustion of carbon, which can be expressed as the following reaction: $Co_8S_9 + 14\ O_2 = 3\ Co_3O_4 + 8\ SO_2$

The final weight change (~6.1%) observed from 450 °C to 600 °C is owing to the burning of carbon in the composite and the partial transformation of Co_3O_4 to $CoSO_4$ phase: $Co_3O_4 + 3\ SO_2 + O_2 = 3\ CoSO_4$

It is difficult to determine the exact phase content of $CoSO_4$ phase, since complex structural related factors (*k* factor) for both the Co_3O_4 and $CoSO_4$ phases should be calculated in advance. Here we use the ratio of integrated intensity to estimate the phase content of $CoSO_4$ phase (~50%) in the composites (Fig. S7c).

Based on the above reaction equations, the weight fraction of carbon in the Co_9S_8@NMCN nanocomposites is calculated to be ca. 47%. The high ratio of carbon is likely to contribute to the advantage of constructing conductive network for enhanced lithium storage properties.

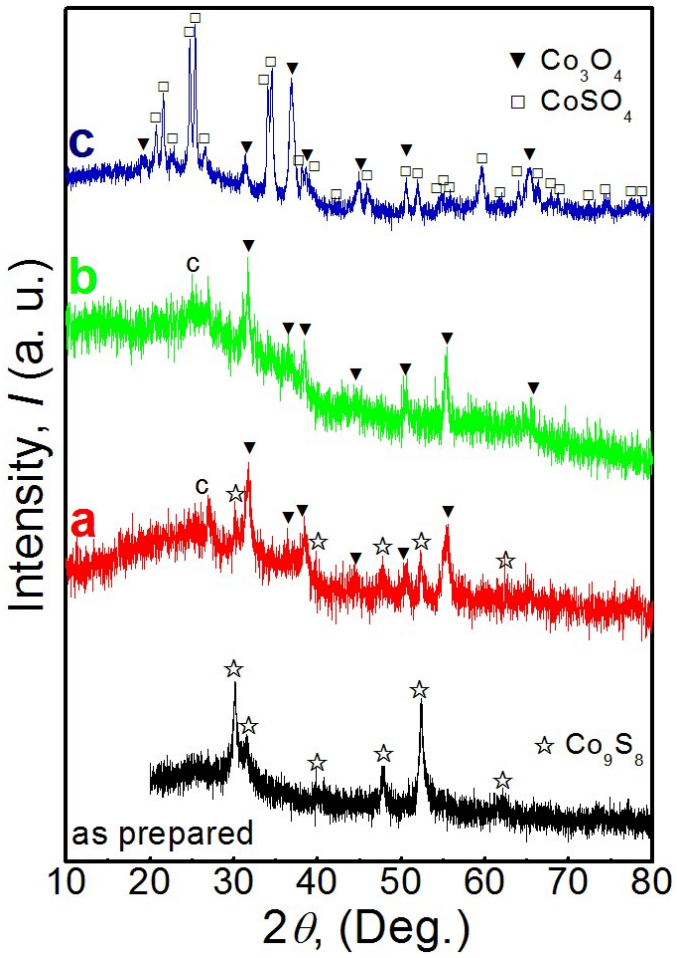

Fig. S7 *Ex-situ* XRD patterns of the products from TGA experiments at different temperatures. (a) 250 °C, (b) 350 °C, (c) 550 °C. The pattern of the as prepared Co_9S_8 is also shown for comparison.

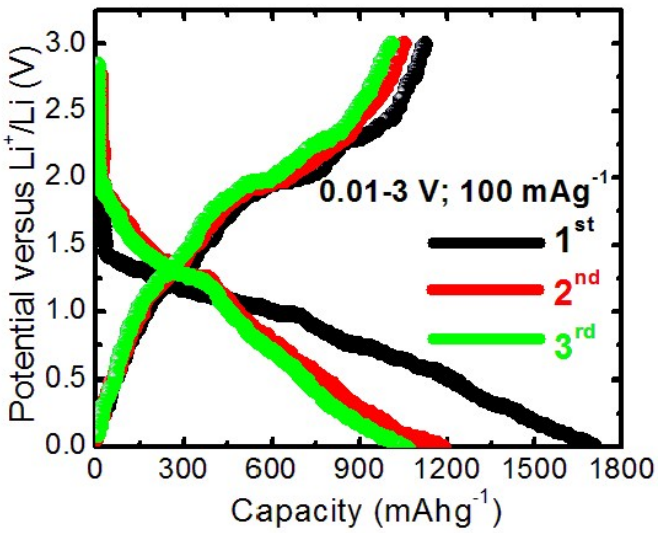

Fig. S8 Charge/discharge curves of the first three cycles for the Co_9S_8@NMCN nanocomposites electrode between 0.01 and 3 V versus Li/Li^+ at a current density of 100 mAg^{-1}.

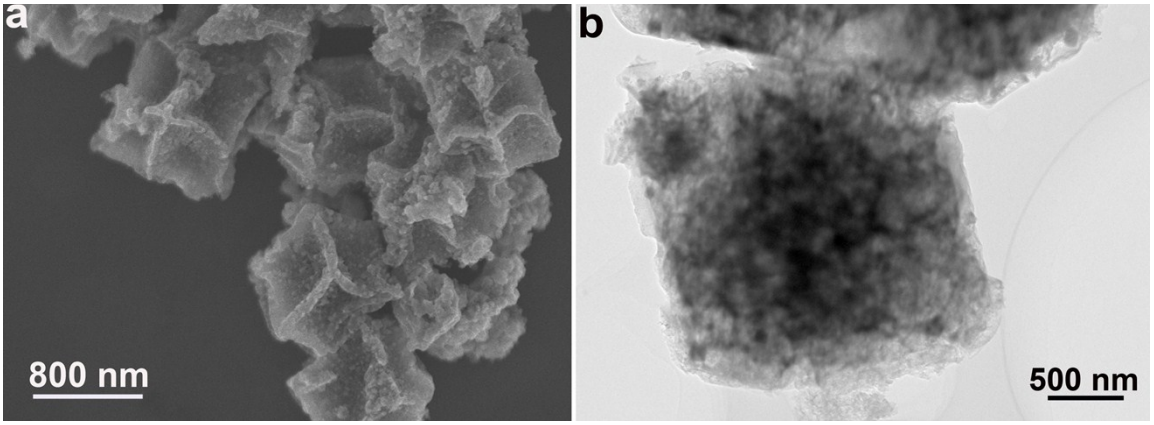

Fig. S9 (a) SEM and (b) TEM images of the Co_9S_8@NMCN nanocomposites electrode after cycling performance testing (80 cycles, current rate 100 mAg^{-1}, 0.01-3 V versus Li/Li^+).